

Cranfield

6 MEI 1991

College of Aeronautics Report No. 9002
November 1989

TECHNISCHE UNIVERSITEIT DELFT
LUCHTVAART- EN RUIMTEVAARTTECHNIEK
BIBLIOTHEEK
Kluyvenweg 1 - 2629 HS DELFT

The Performance of 60° Delta Wings:
The Effects of Leading Edge Radius and Vortex Flaps.

B K Hu and Prof J L Stollery

The Department of Aerodynamics
College of Aeronautics
Cranfield Institute of Technology
Cranfield, Bedford MK43 OAL, England

College of Aeronautics Report No. 9002
November 1989

The Performance of 60° Delta Wings:
The Effects of Leading Edge Radius and Vortex Flaps.

B K Hu and Prof J L Stollery

The Department of Aerodynamics
College of Aeronautics
Cranfield Institute of Technology
Cranfield, Bedford MK43 0AL, England

ISBN 1 871564 03 4

£8.00

*"The views expressed herein are those of the authors alone and do not
necessarily represent those of the Institute"*

SUMMARY

Low-speed wind tunnel tests were conducted on sharp edge flat 60° delta wing, the wing with leading edge vortex flap deflected 30° and 60° delta wing with well rounded leading edge to estimate the effects of leading edge vortex flap and leading edge radius on the aerodynamic performance of 60° delta wings.

Results indicate that the leading edge vortex flap can increase lift/drag ration of up to 19% , well rounded leading edge can increase further lift/drag ratio of up to 39%.

NOTATION

AR	Aspect ratio
C	Wing chord
C_D	Drag coefficient
C_L	Lift coefficient
HL	Hinge line
L/D	Lift/Drag ratio
R_e	Reynolds number (based on wing centreline chord)
α	Wing angle of attack
LEVF	Leading edge vortex flap
δ_{LEVF}	Leading edge vortex flap deflection measured normal to the hinge line

1. INTRODUCTION

At the high angles of attack necessary for take off, landing, and manoeuvre, slender wing planforms with a sharp leading edge designed for supersonic cruise aircraft develop leading edge vortex flow. This separation-induced vortex flow generates nonlinear vortex lift, but it is unfortunately accompanied by a substantial increase in lift induced drag caused by the loss of leading edge suction. The drag penalty associated with leading edge vortex flow can be reduced in a number of ways.

The leading edge of the wing is well rounded in order to maintain attached leading edge flow and thus to prevent vortex formation. It recovers leading edge suction and results in large reduction in the lift induced drag. But the high zero lift drag penalty caused by rounded leading edge at supersonic speeds is unacceptable.

Leading edge vortex flap (LEVF) is a means to generate substantial reduction in lift induced drag by 'capturing' the leading edge vortex along a forward facing deflection surface. The vortex suction acting on the surface can develop a thrust. When the flow reattaches at the LEVF hinge line, an attached lifting flow is provided over the upper surface of the wing. The flap deflection must be such that the flow separates at the edge of the flap and vortex results. The size of the flap must be sufficient to give reattachment at the LEVF hinge line.

The primary purpose of the paper is to estimate the effects of well rounded leading edge and leading edge vortex flap on the aerodynamic performance of 60° delta wings.

A series of tests were made in the Cranfield IA open-jet, low-speed wind tunnel using 60° delta wings made from plywood.

2. EXPERIMENTAL DETAILS

Details of models are given in Fig.1. The models tested have a

leading edge sweep angle of 60° and no camber. The delta 1 model (Fig.1a) having the symmetric aerofoil section has a thickness/chord ratio of 10% which occurs at 35% C and a well rounded leading edge, $R_{LE} = 0.69\% C$. The spanwise thickness distribution varies linearly from root to tip. The delta 2 model (Fig.1b) is a flat delta wing with sharp leading and trailing edges to enhance flow separation. The model incorporated a LEVF hinge line running along rays from the apex to the 75% semispan station at the trailing edge (Fig.1c). The LEVF deflection (δ_{LEVF}) of 30° was tested. It is measured in the plane normal to the hinge line.

Measurements of lift and drag of models were made in the 40" x 27" low-speed open-jet wind tunnel, using a T.E.M. three component wind tunnel balance. All the tests were conducted at a tunnel speed of about 28 m/s. The angle of attack range was from -6° to $+40^\circ$ to include the stall. The Reynolds number based on centreline chord were 0.739×10^6 (delta 1 model) and 0.853×10^6 (delta 2 model).

The model was mounted on twin shielded struts with a tail-sting for angle of attack control.

Prior to testing, the T.E.M. balance was calibrated.

Corrections to the collected data were applied as follows:

A correction to the measured angle of attack due to the constraint of the working section boundaries. This is known as the lift effect and is calculated using the method of images (see Ref.1);

Owing to the angle of attack correction, the lift vector is inclined and so a correction to the measured drag is also required.

Interference between the twin shielded struts and the wing was assumed negligible.

All the force data have been reduced to coefficient form. These coefficients are based on total plan area. Measured angles of attack, lift and drag coefficients along with the corrected values are

presented in tables 1 - 3.

3. RESULTS AND DISCUSSION

The sharp edge flat delta 2 is used as a datum for both delta 1 with well rounded leading edge ($R_{LE} = 0.69\% C$) and delta 2 with leading edge vortex flap deflected 30° tested. Because it would provide a base case with no leading edge suction, hence all leading edge suction found in testing would be the results of the vortex action on the LEVF or well rounded leading edge action.

3.1 Lift

The $C_L - \alpha$ curves are plotted in Figs. 2a and 3a. It is not zero at zero angle of attack ($\alpha_0 = -1.1^\circ$) for sharp edges delta 2. This is due to assymetry in the leading edge equivalent to a slight up-camber.

Fig.2a shows that at $12^\circ < \alpha < 24^\circ$ the delta 1 with well rounded leading edge produces lower values of C_L than the datum delta 2. Increased aerofoil nose radius has a very powerful effect on retarding the development of the leading edge vortex. A large nose radius maintains leading edge attached flow, a leading edge vortex does not form. The delta 2 generates vortex lift. The delta 2 stalls at an angle of attack of 27.7° , while the delta 1 does not stall until an angle of attack of 30° .

Fig.3a shows that at all angles of attack below 33° the delta 2 with LEVF deflected 30° produces lower values of C_L than datum delta 2. Because LEVF deflected 30° produces weaker leading edge vortex than flat sharp edge. The $C_L - \alpha$ curve also shows a progressive reduction of lift curve slope with α for the delta 2 with LEVF deflected 30° . This is due to two effects, a reduction in the projected planform area (whereas the C_L plotted is based on the constant total plan area) and a reduction in the effective aspect ratio.

3.2 Drag

The $C_D - \alpha$ curves are plotted in Figs. 2b and 3b.

Fig. 2b shows that at all angles of attack below 34° the delta 1 produces lower drag than the datum delta 2. Because the delta 1 with well rounded leading edge maintains leading edge attached flow and recovers leading edge suction resulting from flow acceleration around the leading edge. The delta 1 produces lower zero lift drag due to smoother surface than the datum delta 2.

Fig. 3b shows that when the LEVF is deflected 30° the angle of attack at which the drag is a minimum will increase. It moves from about 0.4° to 2° . At $-6^\circ < \alpha < 2^\circ$ the delta 2 with the LEVF deflected 30° produces higher drag than the datum delta 2. At zero angle of attack with the flap deflected a vortex will form on the lower surface of the flap, and the suction acting on the underside of the flap will produce negative lift and increased drag. At $2^\circ < \alpha < 36^\circ$ deflecting the LEVF markedly reduces drag. According to Ref. 2 as the wing angles of attack is increased, a value is reached for which the flow comes smoothly onto the leading edge of the flap deflected 30° . There is attached leading edge flow and no flow separation. At higher angles of attack the leading edge separation occurs, the leading edge vortex forms and strengthens, so the delta 1 with the deflected LEVF produces significantly low lift induced drag.

3.3 Lift/Drag Ratio

The lift/drag ratio is used as a basic aerodynamic performance parameter.

Figs. 2c and 4 illustrate L/D versus C_L on the delta 1, the delta 2 and the delta 2 with the LEVF deflected 30° configurations tested and the effects of leading edge radius and LEVF on L/D . Fig. 2c shows that when $0 < C_L < 0.8$ the delta 1 with leading edge radius $R_{LE} = 0.69\% C$ has higher lift/drag ratio than the datum delta 2. It is clear that well rounded leading edge offers the aerodynamic performance improvements. Because it maintains attached leading edge

flow and produces low drag. Deflecting the LEVF reduces both the lift and the drag but the drag reduction is more significant. Fig.4 shows that the LEVF deflected 30° offers increased lift/drag ratio at a lift coefficient range of about $0.31 \leq C_L < 0.7$.

Comparing lift/drag ratio for the flat delta (delta 2) and the wing with the vortex flap deflected 30° with that for the delta 1 with well rounded leading edge, it is clear that the delta 1 offers the highest lift/drag ratio over the entire C_L range tested. Well rounded leading edge wing improves further aerodynamic performance of 60° delta wings. The percentage improvements in lift/drag ratio (Fig.5) show that the LEVF deflected 30° offers maximum improvement in lift/drag ratio of 19%, while well rounded leading edge offers maximum improvement in lift/drag ratio of 39%.

The experimental data on 60° delta wing with well rounded leading edge at $R_e = 9.28 \times 10^6$ (based on the mean wing chord) given in table 5 of Ref.4 are plotted on Fig.2c. Comparing L/D shows that Ref.4 gives higher lift/drag ratio than our delta 1 (the same wing). This is due to the effect of Reynolds number on lift and drag.

4. CONCLUSIONS

1. 60° delta wing with well rounded leading edge ($R_{LE} = 0.69\% C$) maintains leading edge attached flow. It produces low drag and gives high lift/drag ratio over a wide range of lift coefficient.
2. Leading edge vortex flap deflected 30° gives appreciable improvement in lift/drag ratio at $0.3 < C_L < 0.7$.
3. The leading edge vortex flap deflected 30° reduces both the lift and the drag, but the drag reduction is more significant.
4. Comparing the effect of the sharp leading edge vortex flap deflected 30° with that of the well rounded leading edge on lift/drag ratio, we find that the rounded nose ($R_{LE} = 0.69\% C$) provides further improvement in lift/drag ratio.

REFERENCES

1. Parkhurst, R.C., and Holder, D.W. Wind tunnel technique; an account of experimental methods in low- and high-speed wind tunnels. PITMAN, 1952.
2. Stollery, J.L., and Ellis, D.G. The behaviour and performance of vortex flaps. College of Aeronautics Report No. NFP 8914, November 1989.
3. Ellis, D.G. The behaviour and performance of leading edge vortex flaps. College of aeronautics Report No. 8601, 1986.
4. Jones, R., Miles, C.J.W., and Pursey, P.S. Experiments in the compressed air tunnel on swept-back wings including two delta wings. A.R.C. Technical Report R & M No. 2871, 1954.
5. Kulfan, R.M. Wing geometry effects on leading edge vortices. AIAA 79-1872. August 20-22, 1979.

Date: 20/9/89 p.m.

TABLE 1

Incidence, lift coefficient, drag coefficient (both corrected and uncorrected) and lift/drag ratio for Delta 1.

NO.	α°		C_L		C_D		$L/D(C)$
	$\alpha_{(U)}$	$\alpha_{(C)}$	$C_{L(U)}$	$C_{L(C)}$	$C_{D(U)}$	$C_{D(C)}$	
1	-6	- 5.630	- 0.248	- 0.248	0.045	0.043	-
2	-4	- 3.756	- 0.164	- 0.164	0.035	0.034	-
3	-2	- 1.890	- 0.074	- 0.074	0.021	0.021	-
4	0	- 0.009	0.006	0.006	0.018	0.018	0.333
5	2	1.855	0.097	0.097	0.020	0.020	4.850
6	4	3.708	0.196	0.196	0.022	0.021	9.333
7	6	(5.508)	(0.33)	(0.33)	(0.033)	(0.03)	(11.000)
		5.580	0.282	0.282	0.032	0.030	9.400
8	8	7.382	0.415	0.415	0.046	0.042	9.881
9	10	9.270	0.490	0.490	0.063	0.057	8.596
10	12	11.151	0.570	0.571	0.088	0.080	7.138
11	14	13.033	0.649	0.650	0.117	0.106	6.132
12	16	14.924	0.722	0.723	0.153	0.140	5.164
13	18	16.833	0.783	0.784	0.206	0.190	4.126
14	20	18.762	0.831	0.832	0.252	0.234	3.556
15	22	20.652	0.905	0.906	0.301	0.280	3.236
16	24	22.543	0.978	0.979	0.356	0.331	2.958
17	26	24.434	1.051	1.052	0.407	0.379	2.776
18	28	26.351	1.107	1.108	0.466	0.435	2.547
19	30	28.318	1.129	1.130	0.535	0.502	2.251
20	32	30.300	1.141	1.142	0.583	0.550	2.076
21	34	32.334	1.118	1.119	0.625	0.593	1.887
22	36	34.361	1.100	1.101	0.646	0.615	1.790
23	38	36.477	1.022	1.023	0.656	0.629	1.626
24	40	38.631	0.919	0.920	0.638	0.617	1.491

Date: 21/9/89 p.m.

TABLE 1 (continued)
(Repeated test)

NO.	α°		C_L		C_D		$L/D(C)$
	$\alpha_{(U)}$	$\alpha_{(C)}$	$C_{L(U)}$	$C_{L(C)}$	$C_{D(U)}$	$C_{D(C)}$	
1	-6	- 5.665	- 0.225	- 0.225	0.035	0.034	-
2	-4	- 3.794	- 0.138	- 0.138	0.021	0.021	-
3	-2	- 1.909	- 0.061	- 0.061	0.017	0.017	-
4	0	- 0.043	0.029	0.029	0.017	0.017	1.706
5	2	1.823	0.119	0.119	0.021	0.021	5.667
6	4	3.693	0.206	0.206	0.026	0.025	8.240
7	6	5.593	0.273	0.273	0.034	0.032	8.531
8	8	7.473	0.354	0.354	0.047	0.044	8.045
9	10	9.349	0.437	0.437	0.065	0.060	7.283
10	12	11.203	0.535	0.536	0.093	0.086	6.233
11	14	13.085	0.614	0.615	0.125	0.115	5.348
12	16	14.967	0.693	0.694	0.161	0.149	4.658
13	18	16.848	0.773	0.774	0.205	0.190	4.074
14	20	18.757	0.834	0.835	0.247	0.229	3.646
15	22	20.668	0.894	0.895	0.299	0.279	3.208
16	24	22.574	0.957	0.958	0.360	0.337	2.843
17	26	24.531	0.986	0.987	0.415	0.390	2.531
18	28	26.443	1.045	1.046	0.471	0.443	2.361
19	30	28.403	1.072	1.073	0.531	0.502	2.137
20	32	30.382	1.086	1.087	0.585	0.555	1.959
21	34	32.438	1.048	1.049	0.633	0.605	1.734
22	36	34.506	1.003	1.004	0.640	0.614	1.635
23	38	36.573	0.958	0.959	0.655	0.632	1.517
24	40	38.634	0.917	0.918	0.650	0.629	1.459

Date: 19/9/89 p.m.

TABLE 2

Incidence, lift coefficient, drag coefficient (both corrected and uncorrected) and lift/drag ratio for Delta 2.

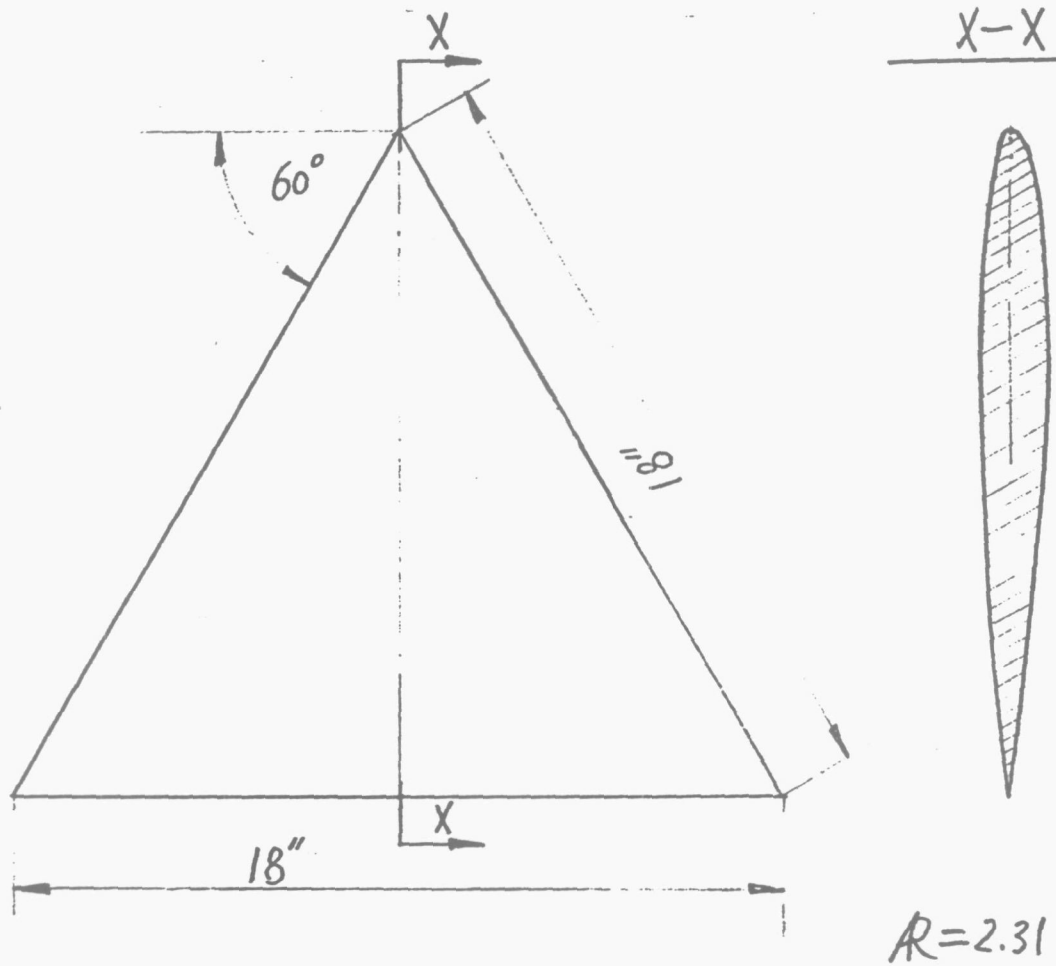
NO.	α°		C_L		C_D		$L/D(C)$
	$\alpha_{(U)}$	$\alpha_{(C)}$	$C_{L(U)}$	$C_{L(C)}$	$C_{D(U)}$	$C_{D(C)}$	
1	-6	- 5.587	- 0.212	- 0.212	0.060	0.059	-
2	-4	- 3.774	- 0.116	- 0.116	0.048	0.048	-
3	-2	- 1.940	- 0.031	- 0.031	0.034	0.034	-
4	0	- 0.109	0.056	0.056	0.028	0.028	2.000
5	2	1.741	0.133	0.133	0.029	0.028	4.750
6	4	3.569	0.221	0.221	0.032	0.030	7.367
7	6	5.427	0.294	0.294	0.039	0.036	8.167
8	8	7.258	0.381	0.381	0.055	0.050	7.620
9	10	9.073	0.476	0.476	0.075	0.067	7.104
10	12	10.851	0.590	0.591	0.114	0.102	5.794
11	14	12.738	0.648	0.649	0.149	0.135	4.807
12	16	14.568	0.735	0.736	0.186	0.168	4.381
13	18	16.436	0.803	0.804	0.231	0.209	3.847
14	20	18.303	0.871	0.872	0.283	0.257	3.393
15	22	20.179	0.935	0.936	0.343	0.314	2.981
16	24	22.031	1.011	1.012	0.414	0.380	2.663
17	26	23.986	1.034	1.035	0.463	0.427	2.424
18	28	25.898	1.079	1.080	0.528	0.499	2.163
19	30	27.836	1.111	1.112	0.580	0.539	2.063
20	32	29.859	1.099	1.100	0.634	0.594	1.852
21	34	31.939	1.058	1.059	0.665	0.628	1.686
22	36	34.165	0.942	0.943	0.658	0.628	1.502
23	38	36.385	0.829	0.830	0.601	0.578	1.436
24	40	38.453	0.794	0.795	0.597	0.576	1.380

Date: 27/9/89 p.m.

TABLE 3

Incidence, lift coefficient, drag coefficient (both corrected and uncorrected) and lift/drag ratio for Delta 2 with LEVF. $\delta_{LEVF} = 30^\circ$.

NO.	α°		C_L		C_D		$L/D(C)$
	$\alpha_{(U)}$	$\alpha_{(C)}$	$C_{L(U)}$	$C_{L(C)}$	$C_{D(U)}$	$C_{D(C)}$	
1	-6	- 5.482	- 0.266	- 0.266	0.069	0.067	-
2	-4	- 3.634	- 0.188	- 0.188	0.051	0.050	-
3	-2	- 1.776	- 0.115	- 0.115	0.039	0.039	-
4	0	0.084	- 0.043	- 0.043	0.033	0.033	-
5	2	1.940	0.031	0.031	0.025	0.025	1.240
6	4	3.776	0.115	0.115	0.027	0.027	4.259
7	6	5.649	0.180	0.180	0.031	0.030	6.000
8	8	7.494	0.260	0.260	0.037	0.035	7.429
9	10	9.347	0.335	0.335	0.044	0.040	8.375
10	12	11.223	0.399	0.399	0.051	0.044	9.068
11	14	13.082	0.471	0.471	0.066	0.059	7.983
12	16	14.940	0.544	0.545	0.088	0.078	6.987
13	18	16.788	0.622	0.623	0.115	0.102	6.108
14	20	18.646	0.695	0.696	0.164	0.148	4.703
15	22	20.516	0.762	0.763	0.209	0.189	4.037
16	24	22.379	0.832	0.833	0.258	0.235	3.545
17	26	24.241	0.903	0.904	0.306	0.278	3.252
18	28	26.130	0.960	0.961	0.362	0.331	2.903
19	30	28.060	0.996	0.997	0.432	0.399	2.499
20	32	30.003	1.025	1.026	0.496	0.461	2.226
21	34	32.013	1.020	1.021	0.553	0.518	1.971
22	36	34.023	1.015	1.016	0.576	0.542	1.875
23	38	36.101	0.975	0.976	0.622	0.590	1.654
24	40	38.175	0.937	0.938	0.608	0.579	1.620



Ordinates of Wing Section in Terms of Chord

Distance from leading edge	Height above chord $\times 100$	Distance from leading edge	Height above chord $\times 100$
0	0	0.40	4.96
0.005	0.825	0.45	4.77
0.0075	1.008	0.50	4.49
0.0125	1.300	0.55	4.15
0.025	1.821	0.60	3.75
0.050	2.53	0.65	3.32
0.075	3.04	0.70	2.86
0.100	3.44 _s	0.75	2.39
0.15	4.05	0.80	1.92
0.20	4.47 _s	0.85	1.43 _s
0.25	4.76	0.90	0.95
0.30	4.93 _s	0.95	0.48
0.35	5.00	1.0	0

Nose radius = $0.0069 \times \text{chord}$

Figure 1a. Delta 1 model details

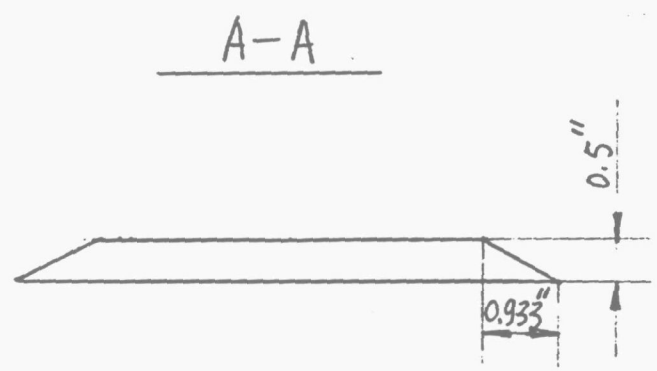
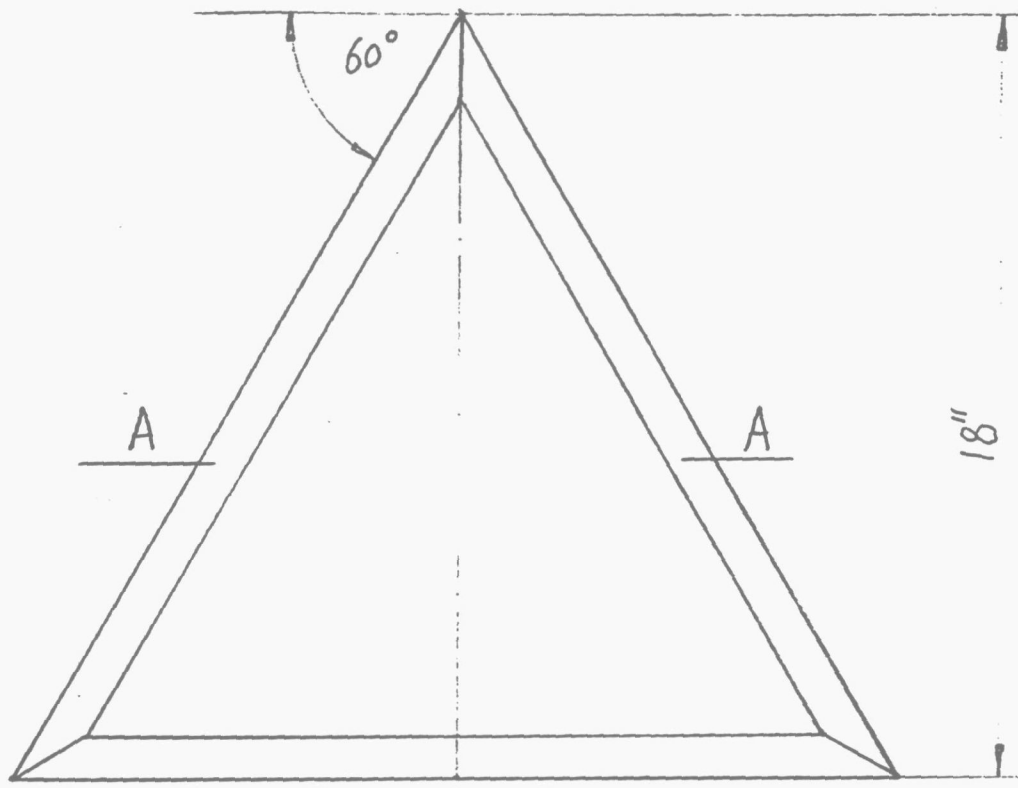
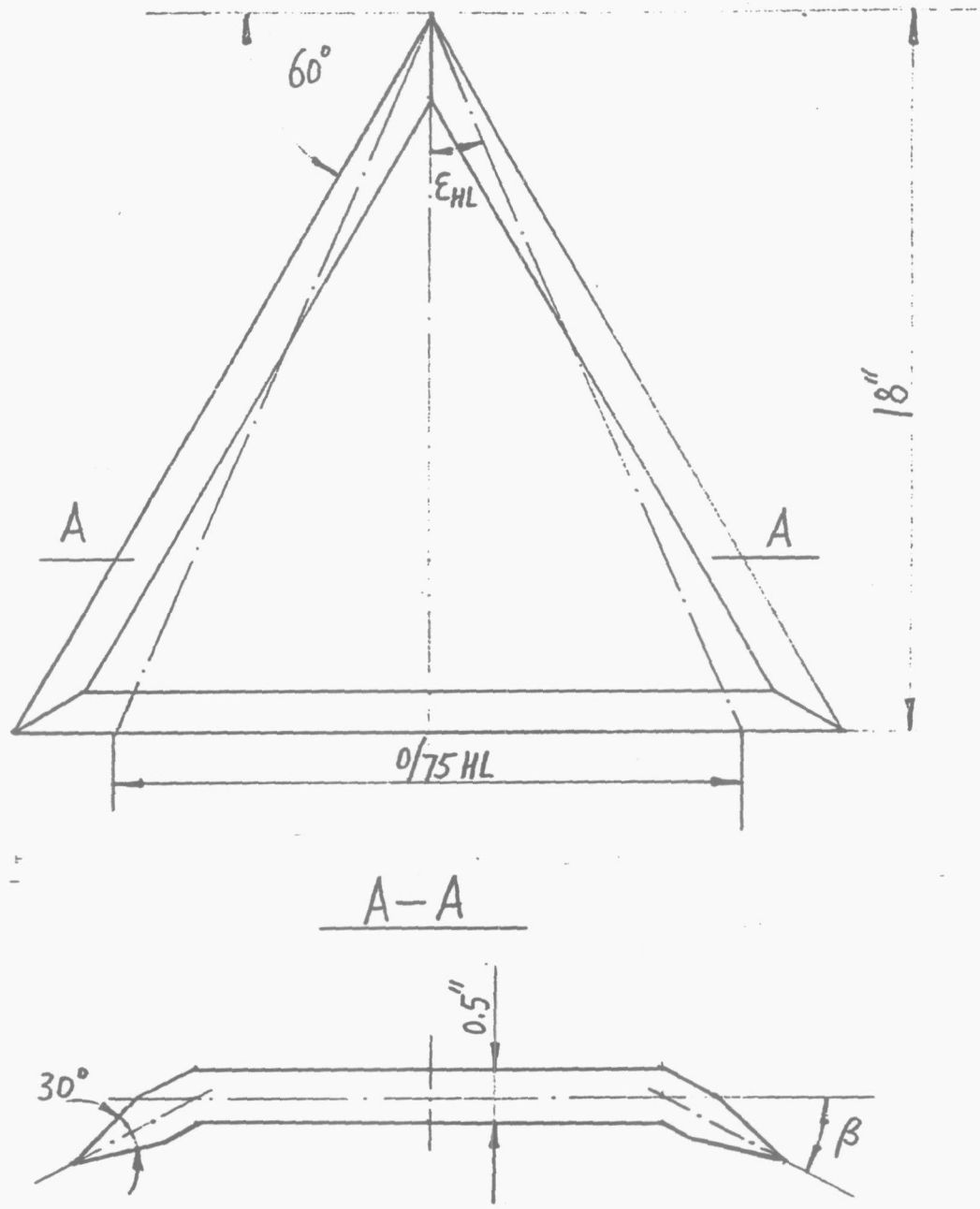


Figure 1b. Delta 2 model details



$SLEVF = 30^\circ$
 SLEVF is measured in a plane perpendicular
 to LEVF hinge line.
 β is measured in the crossflow plane.
 $\beta = \cos \epsilon_{HL} \cdot SLEVF$.

Figure 1c. Delta 2 with LEVF model details

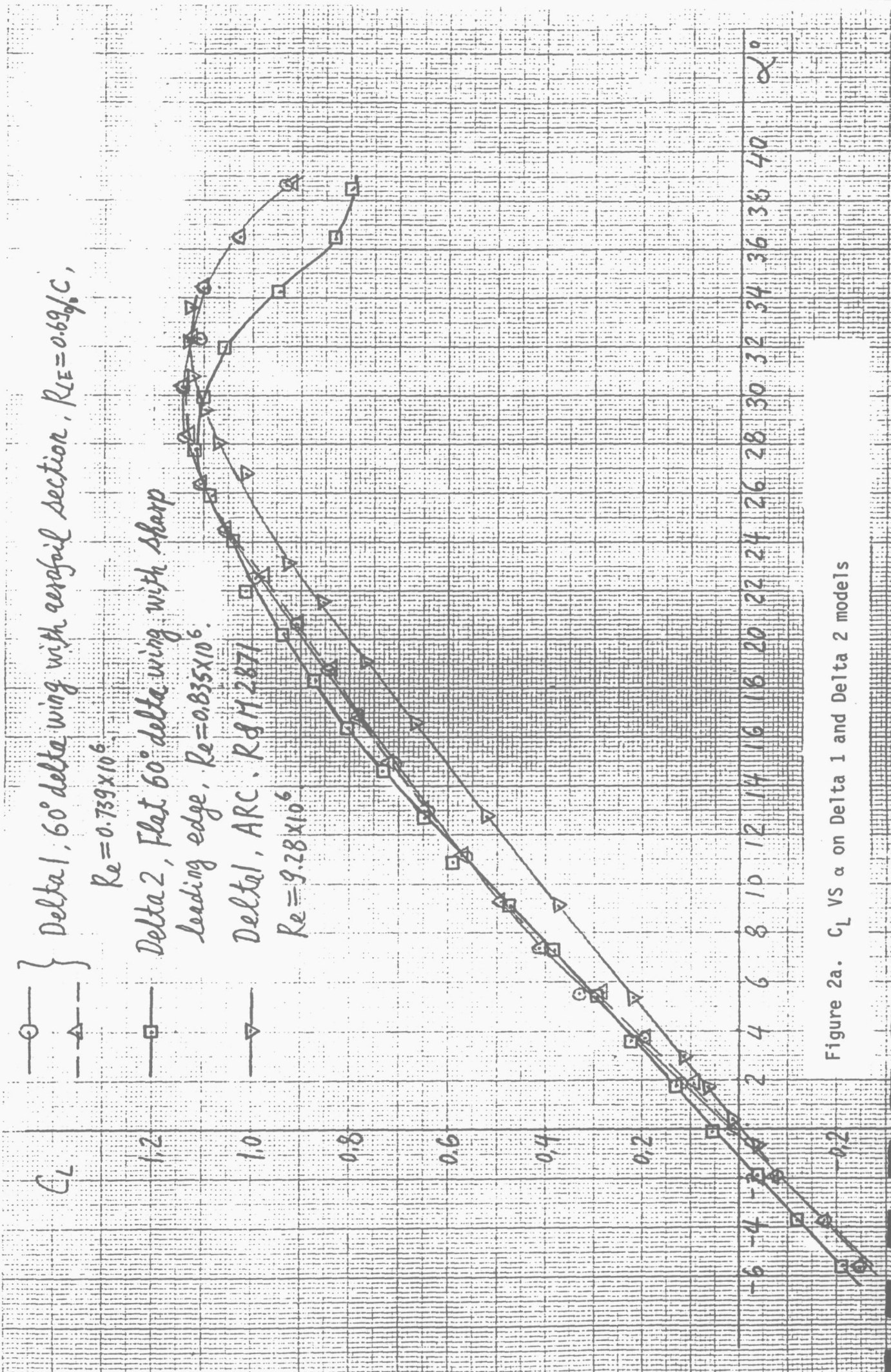


Figure 2a. C_L VS α on Delta 1 and Delta 2 models

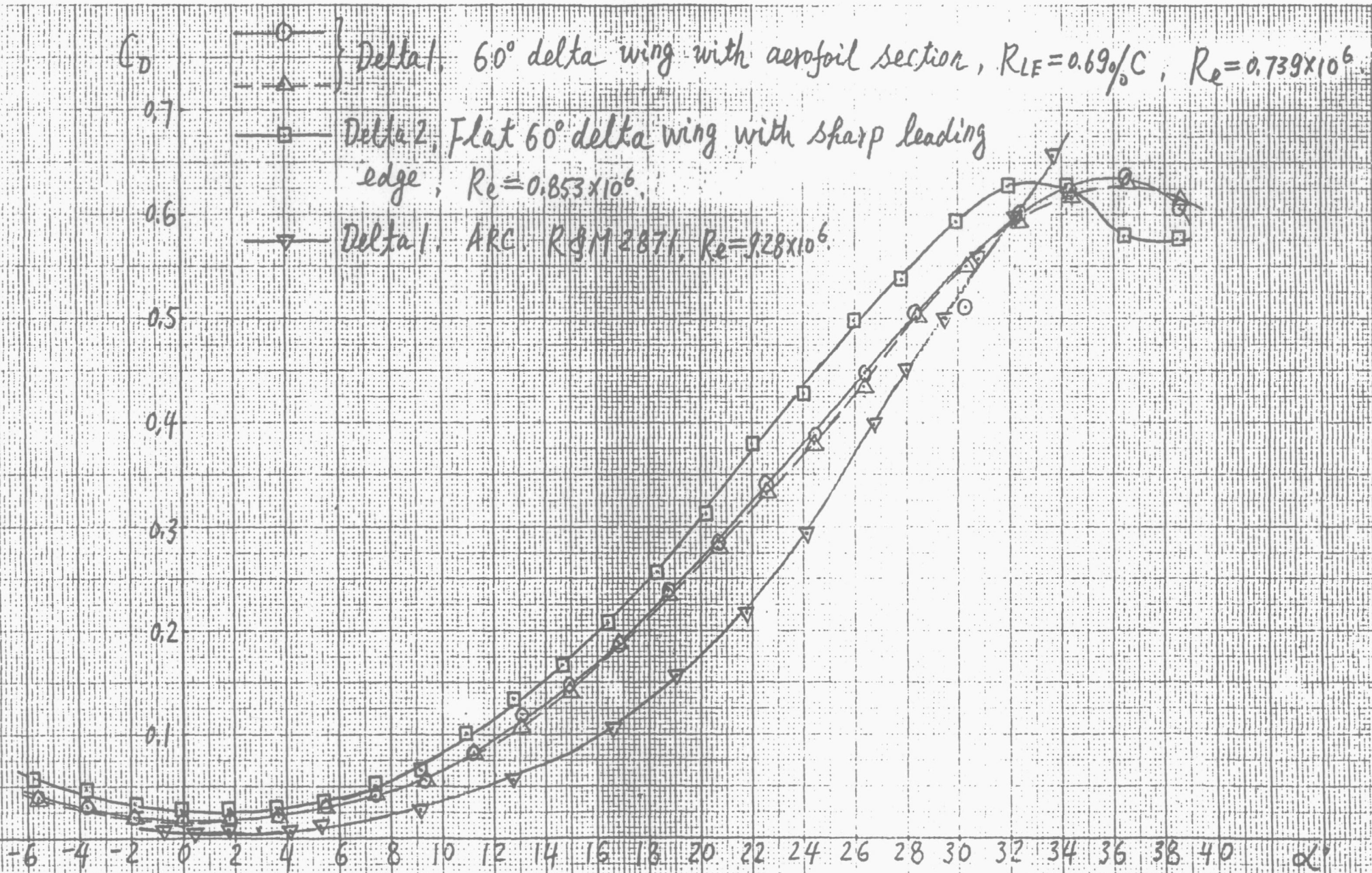


Figure 2b. C_D VS α on Delta 1 and Delta 2 models

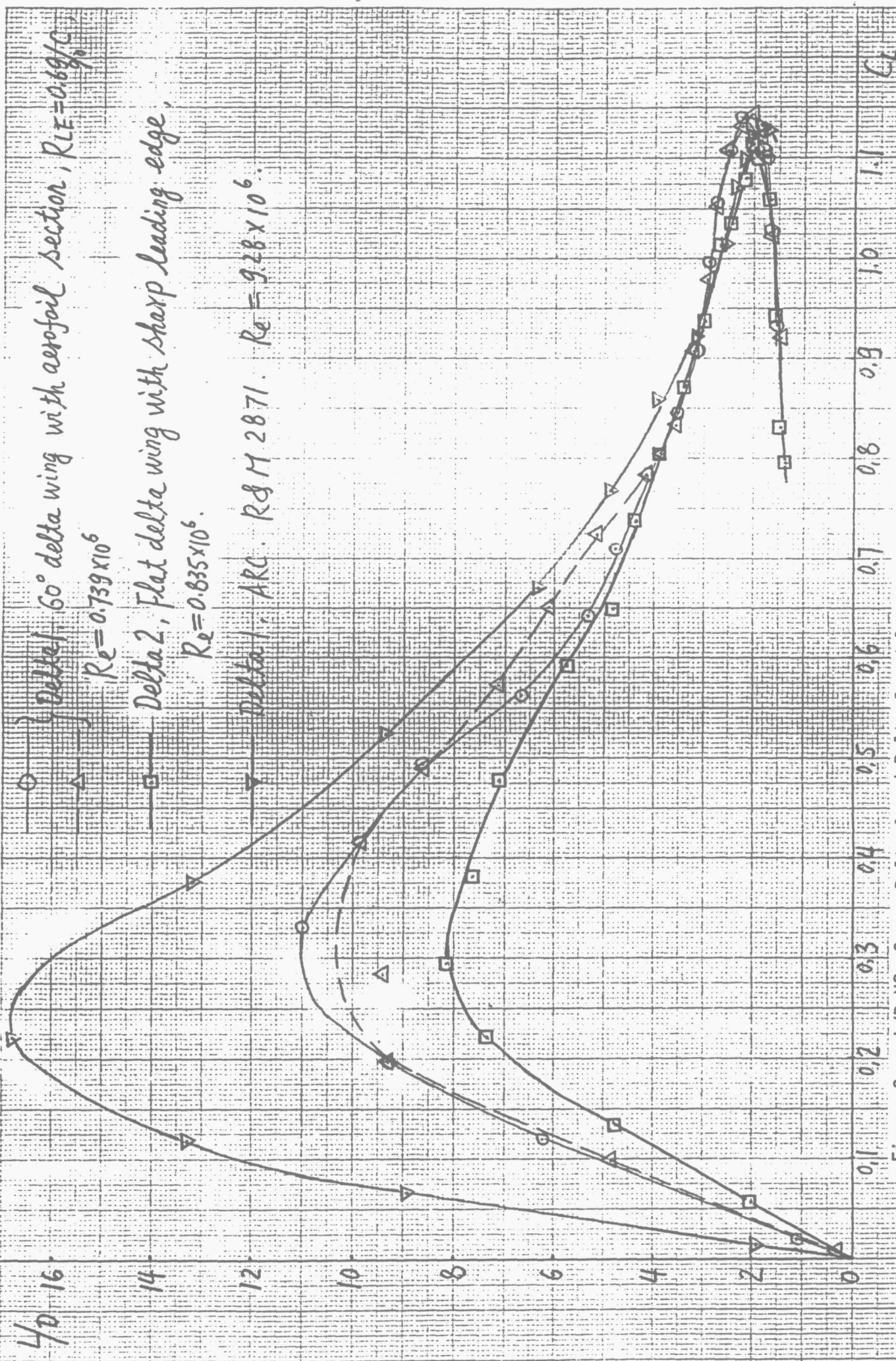


Figure 2c. L/D VS. C_L on Delta 1 and Delta 2 models

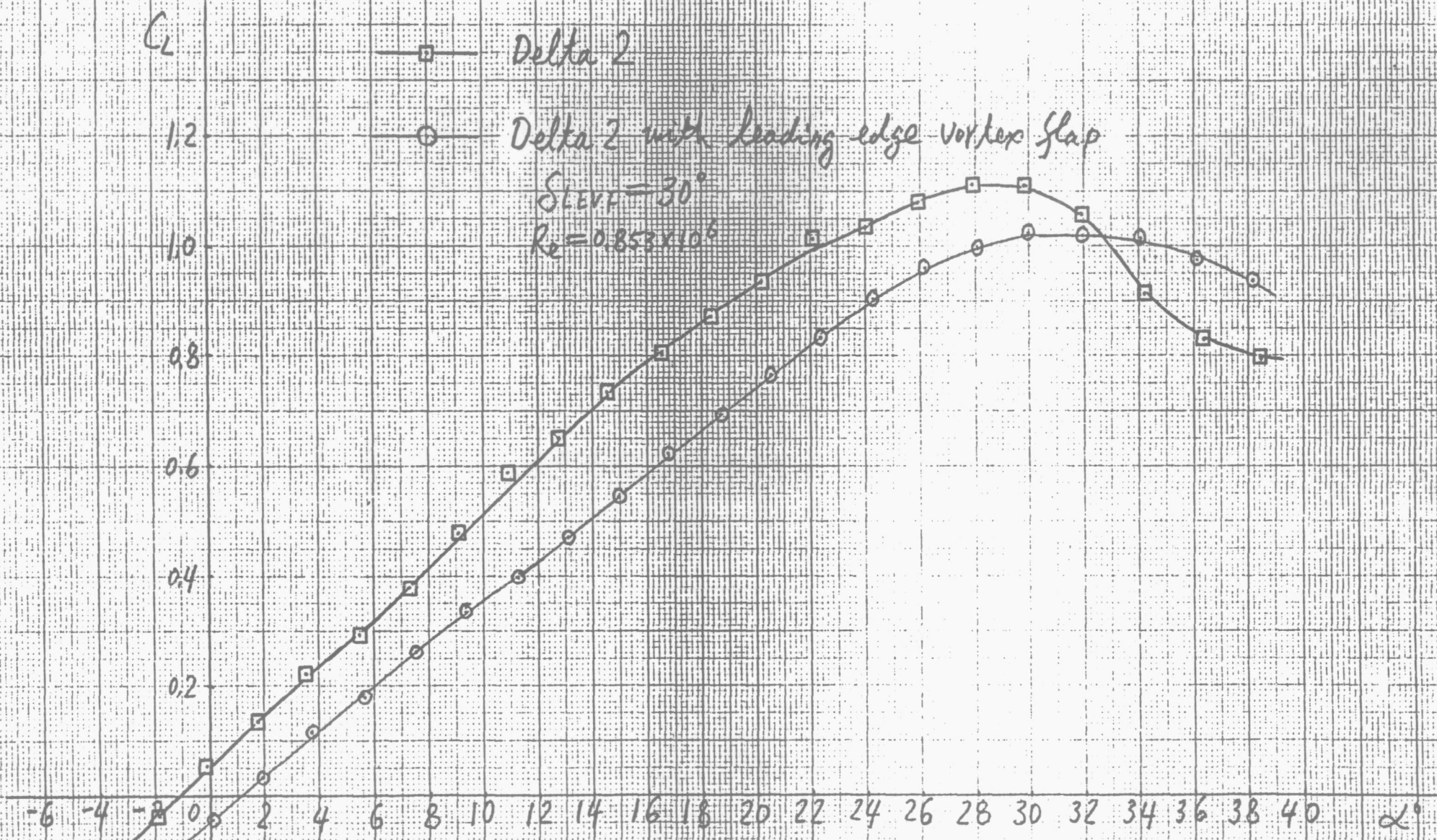


Figure 3a. The effect of LEVF on C_L VS α

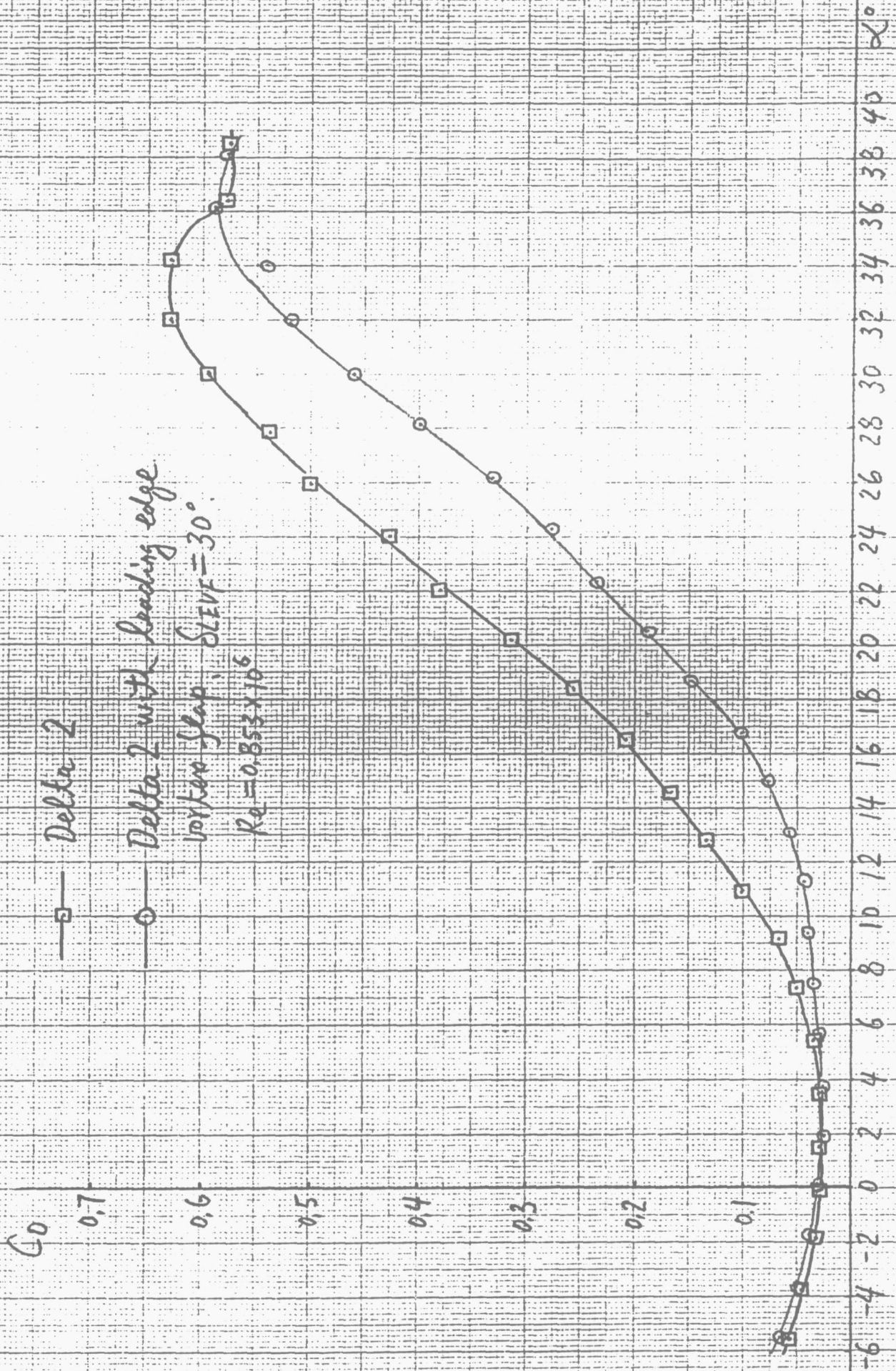


Figure 3b. The effect of LEVF on C_D VS α

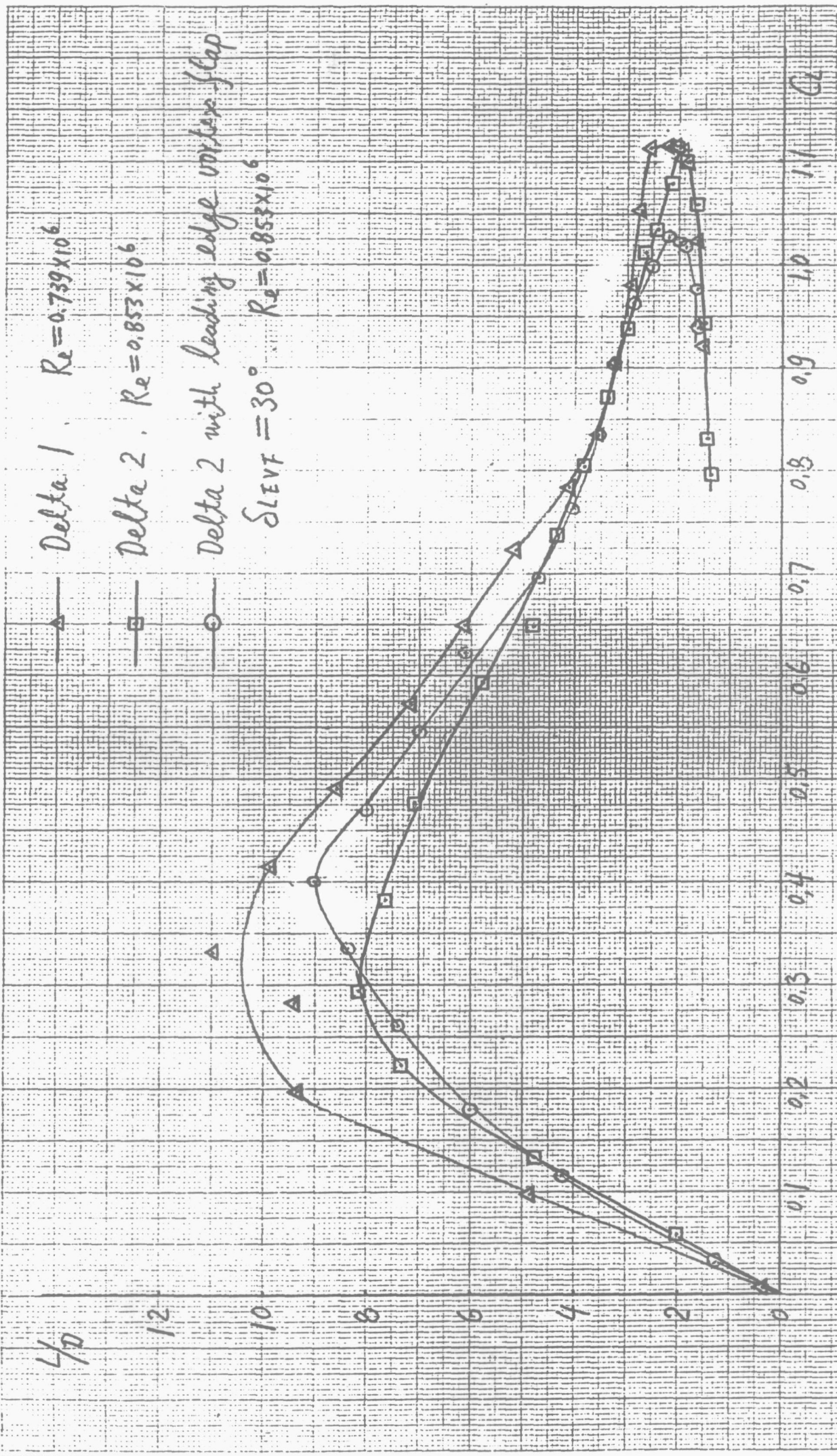


Figure 4. The effect of leading edge shape and LEVF on L/D

Delta 2 with $\delta_{LEVF} = 30^\circ$

Delta 1 (rounding leading edge)

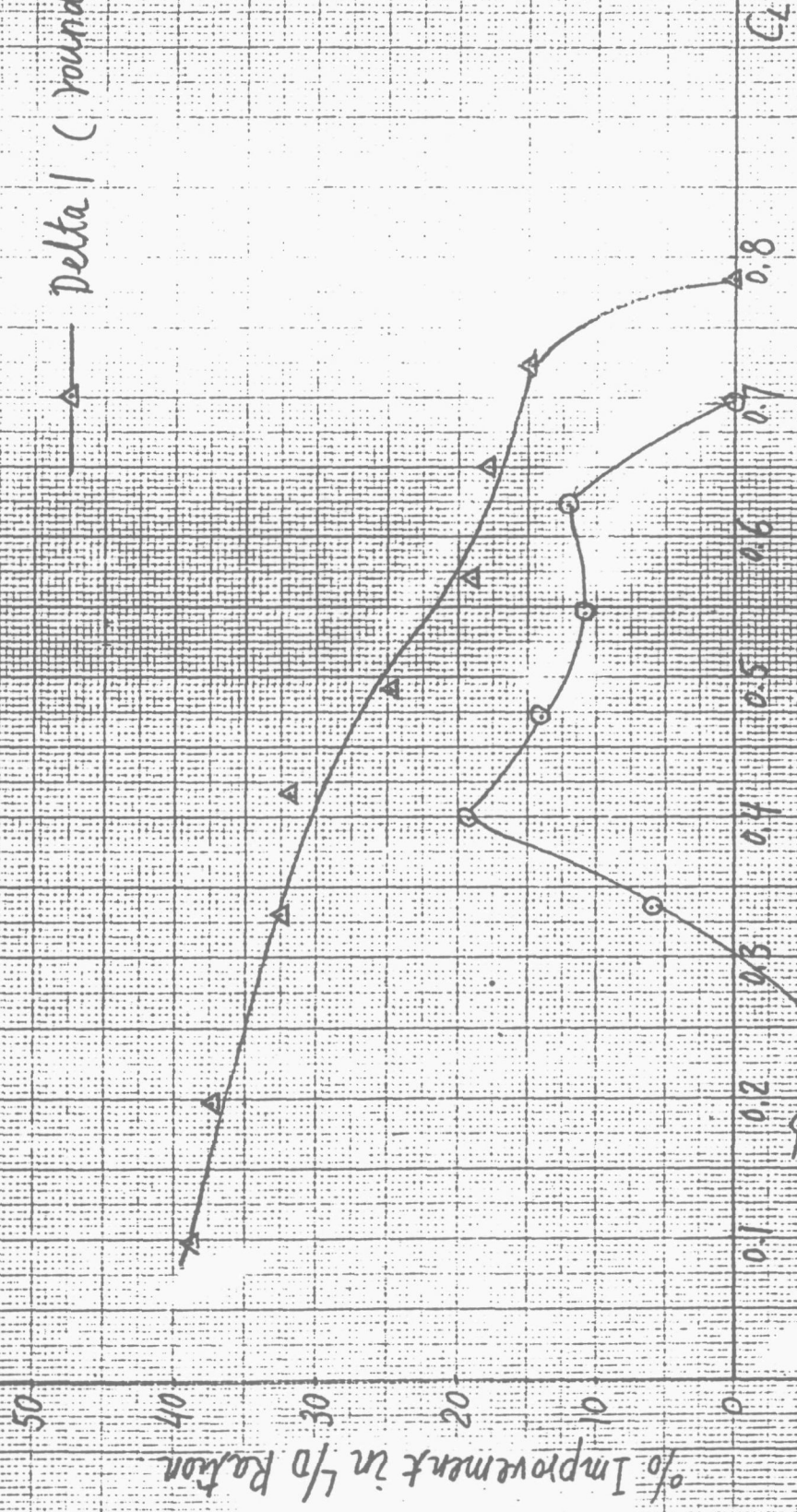


Figure 5. % Improvement in lift/drag ratio VS C_L for $\delta_{LEVF} = 30^\circ$ and rounding leading edge.